Performance Analysis of Reconfigurable Intelligent Surfaces over Nakagami-m Fading Channels

Monjed H. Samuh and Anas M. Salhab, *Senior Member, IEEE*

Abstract—This letter studies the performance of reconfigurable intelligent surface (RIS)-aided networks over Nakagami-m fading channels. First, we derive accurate closed-form approximations for the system channel distributions, and then, use them in deriving closed-form approximations for the outage probability, average symbol error probability (ASEP), and the average channel capacity. In addition, to get more insights at the system performance, we derive asymptotic expression for the outage probability at the high signal-to-noise ratio (SNR) regime, and provide closed-form expressions for the system diversity order and coding gain. Results show that the considered RIS scenario can provide a diversity order of $\frac{a+1}{2}$, where a is a function of the Nakagami-m fading parameter m and the number of reflecting elements N. Furthermore, results illustrate that m is more impactful on the diversity order and the system performance than N. Finally, the provided results are valid for arbitrary number of reflecting elements N and non-integer m.

Index Terms—Reconfigurable intelligent surface, Nakagami-m distribution, accurate approximations.

I. INTRODUCTION

The reconfigurable intelligent surfaces (RISs) have recently attracted noticeable attention as a promising candidate for future wireless communication networks. An RIS is an artificial surface, made of electromagnetic material, that is capable of customizing the propagation of the radio waves impinging upon it [1], [2]. It has been proposed as a new low-cost and less complicated solution to realize wireless communication with high spectrum and energy efficiencies.

The RIS research topic has recently attracted many researchers to investigate it from various aspects. In [3], an overview of the basic characteristics of the large intelligent surface/antenna technology and its potential applications has been provided. A detailed overview on the state-of-the-art solutions, fundamental differences of RIS with other technologies, and the most important open research issues in this area of research has been provided in [4].

The authors in [5] showed that RIS has better performance than conventional massive multiple-input multiple-output (MIMO) systems as well as better performance than multi-antenna amplify-and-forward (AF) relaying networks with smaller number of antennas, while reducing the system complexity and cost. Recently, Yang *et al.* studied in [6] the performance of RIS-assisted mixed indoor visible light

Monjed H. Samouh is with the Department of Applied Mathematics & Physics, Palestine Polytechnic University, Hebron, Palestine (e-mail: monjed-samuh@ppu.edu).

Anas M. Salhab is with the Department of Electrical Engineering, King Fahd University of Petroleum & Minerals, Dhahran 31261, Saudi Arabia (e-mail: salhab@kfupm.edu.sa).

communication (VLC)/radio frequency (RF) system. They derived closed-form expressions for the outage probability and bit error rate (BER) for AF and decode-and-forward (DF) relaying schemes. A study that compares the performance of relay-assisted and RIS-assisted wireless networks from coverage, probability of signal-to-noise ratio (SNR) gain, and delay outage rate has been provided in [7].

The outage probability and BER performance of a dual-hop mixed free space optical (FSO)-RF relay network with RIS has been studied in [8]. In [9], the authors utilized RIS to improve the quality of a source signal, which is sent to destination through an unmanned aerial vehicle (UAV). Tight approximations have been derived for the outage probability, BER, and channel capacity in this paper. The average BER of a RIS-assisted network with space-shift keying (SSK) has been recently studied in [10]. In [11], analytical expression has been derived for the secrecy outage probability of RIS-assisted network in the presence of direct link and eavesdropper.

It is worthwhile to mention here that most of the previous works on RIS-assisted networks performed their analysis based on the central limit theorem (CLT), which means that it is only applicable for a large number of reflecting elements. Following other approach and to cover the case of low number of reflecting elements, the authors in [12] have derived accurate approximations for the channel distributions and performance metrics of RIS-assisted networks assuming Raleigh fading channels. Another paper that derived closed-form expressions for the outage probability, symbol error rate, and ergodic capacity of RIS-assisted networks was presented in [13]. The authors compared the performance of RIS-assisted scenario with AF relaying assuming Rayleigh fading channels. Most recently, [14] provided closed-form expressions for the bit error probability of RIS-assisted network over Nakagami-m fading channels. As claimed by the authors, their results are valid only for BPSK and M-QAM modulation techniques.

Although the authors in [14] considered Nakagami-m fading channels, they only derived exact expressions for the error probability for limited number of reflecting elements. In addition, they derived their approximate expressions and bounds for two specific modulation schemes as mentioned before. Furthermore, no insights at the system performance at high SNR values were provided in that study. Motivated by this, we derive in this paper the channel distributions of RIS-assisted networks assuming Nakagami-m fading model using Laguerre series method [15]. We then utilize the achieved SNR statistics in deriving accurate approximations for the system outage probability, average symbol error probability (ASEP), and the average channel capacity. The derived expressions are

valid for arbitrary number of reflecting elements N and non-integer values of fading parameter m. In addition, in order to get more insights at the system performance, we derive closed-form expression for the asymptotic outage probability at high SNR values, where the system diversity order and coding gain are provided and analyzed. To the best of authors' knowledge, the derived expressions are new in an RIS-aided wireless system context and can be useful in future studies due to their tightness and simplicity, as will be shown later in numerical results section.

II. SYSTEM AND CHANNEL MODELS

It is shown in [2] that the maximized end-to-end (e2e) signal-to-noise ratio (SNR) of RIS-assisted networks can be obtained as follows

$$\gamma = \frac{\left(\sum_{i=1}^{N} \alpha_i \beta_i\right)^2 E_s}{N_0} = \bar{\gamma} Z^2, \qquad (1)$$

where α_i and β_i are independently Nakagami-m distributed random variables with shape parameter m and scale parameter Ω (second moment or mean power), E_s is the average power of the transmitted signal, N_0 is the noise power that is assumed to be additive white Gaussian noise with zero mean, N is the number of reflecting elements, and $\bar{\gamma}$ is the average SNR. The direct link between the source and destination is assumed to be blocked due to natural or man-made obstacles. For more details on the channel model, one can refer to [2].

In the following, some statistical characterizations of γ are presented.

Theorem 1: The probability density function (PDF) and the cumulative distribution function (CDF) of the e2e SNR γ in RIS-assisted network assuming Nakagami-m fading model can be, respectively given by

$$f_\gamma(\gamma) \simeq \frac{\left(\frac{\gamma}{\bar{\gamma}}\right)^{\frac{a}{2}} \exp\left(-\frac{\sqrt{\frac{\gamma}{\bar{\gamma}}}}{b}\right)}{2b^{a+1}\Gamma(a+1)\sqrt{\bar{\gamma}\gamma}}, \qquad (2)$$

and

$$F_\gamma(\gamma) \simeq \frac{\gamma\left(a+1, \frac{\sqrt{\frac{\gamma}{\bar{\gamma}}}}{b}\right)}{\Gamma(a+1)}, \qquad (3)$$

where $\gamma(\cdot,\cdot)$ is the lower incomplete gamma function [16, Eq. (8.350.1)],

$$a = \frac{(N+1)\Gamma\left(m+\frac{1}{2}\right)^4 - m^2\Gamma(m)^4}{m^2\Gamma(m)^4 - \Gamma\left(m+\frac{1}{2}\right)^4}, \qquad (4)$$

and

$$b = \frac{m\Omega\left(\Gamma(m)^2\Gamma(m+1)^2 - \Gamma\left(m+\frac{1}{2}\right)^4\right)}{\Gamma\left(m+\frac{1}{2}\right)^2 \Gamma(m+1)^2}. \qquad (5)$$

Proof: Let $Z_i = \alpha_i\beta_i$ be the product of two Nakagami-m random variables. It can be shown that the PDF of Z_i is given by

$$f_{Z_i}(z) = \frac{4\left(\frac{m}{\Omega}\right)^{2m}}{\Gamma(m)^2} z^{2m-1} K_0\left(2\frac{m}{\Omega}z\right), \qquad (6)$$

where $K_\nu(\cdot)$ is the modified ν-order Bessel function of the second kind [16, Eq. (8.432)]. Moreover, the mean and variance of Z_i are, respectively given by $E(Z_i) = \frac{m\Omega\Gamma\left(m+\frac{1}{2}\right)^2}{\Gamma(m+1)^2}$ and $Var(Z_i) = \Omega^2\left(1 - \frac{\Gamma\left(m+\frac{1}{2}\right)^4}{m^2\Gamma(m)^4}\right)$. Now, according to [15, Sec. 2.2.2], the PDF of $Z = \sum_{i=1}^{N} Z_i$ can be tightly approximated by the first term of a Laguerre expansion. The values of a and b are related to the mean and variance of Z as

$$a = \frac{(E(Z))^2}{Var(Z)} - 1, \qquad (7)$$

and

$$b = \frac{Var(Z)}{E(Z)}. \qquad (8)$$

Therefore, the PDF of Z can be formulated as

$$f_Z(z) = \frac{z^a}{b^{a+1}\Gamma(a+1)} \exp\left(-\frac{z}{b}\right). \qquad (9)$$

After performing a transformation of random variables, the PDF of γ is given by (2). Accordingly, the CDF of γ can be obtained from

$$F_\gamma(\gamma) = \int_0^\gamma f_\gamma(x)dx. \qquad (10)$$

The integral is evaluated by substitution and employing [16, Eq. (8.350.1)]. This concludes the proof. ∎

III. PERFORMANCE ANALYSIS

A. Outage Probability

The outage probability is defined as the probability that the e2e SNR goes below a predetermined outage threshold γ_{out}, i.e. $P_{\text{out}} = \Pr\left[\gamma \leq \gamma_{\text{out}}\right]$, where $\Pr[.]$ is the probability operation and γ_{out} is a predetermined outage threshold. Thus, using (3), we have

$$P_{\text{out}} = F_\gamma(\gamma_{\text{out}}). \qquad (11)$$

To get more insights at the system performance, we derive here simple, but accurate closed-form expression for the outage probability at high values of average SNR ($\bar{\gamma} \to \infty$). At the high SNR regime, P_{out} can be represented as $P_{\text{out}} = (G_c\bar{\gamma})^{-G_d}$, where G_c and G_d are the coding gain and diversity order of the system, respectively [18]. By the use of [16, Eq. (8.354.1)], the outage probability can be evaluated at high SNR values as

$$P_{\text{out}}^\infty \simeq \frac{\sum_{n=0}^\infty \frac{(-1)^n \left(\sqrt{\frac{\gamma_{\text{out}}}{\bar{\gamma}}}\right)^{a+n+1}}{(a+n+1)b^{a+n+1}}}{\Gamma(a+1)}. \qquad (12)$$

As $\bar{\gamma} \to \infty$, the first term in the summation in (12) is dominating the other terms. Hence, after considering that term only and with some simple manipulations, (12) simplifies to

$$P_{\text{out}}^\infty \simeq \left[\frac{b^2}{\gamma_{\text{out}}[(a+1)!]^{-\frac{2}{(a+1)}}}\bar{\gamma}\right]^{-\frac{(a+1)}{2}}. \qquad (13)$$

Clearly, we can see from (13) that the coding gain of the system is $G_c = \frac{b^2}{\gamma_{\text{out}}[(a+1)!]^{-\frac{2}{(a+1)}}}$ and the diversity order is $G_d = \frac{a+1}{2}$. In addition, we can see that for Rayleigh fading

$$P_e = \frac{pq^{-\frac{a}{2}-1}\left(\frac{1}{b\sqrt{\bar{\gamma}}}\right)^a \left((a+2)b\sqrt{\bar{\gamma}}\sqrt{q}\Gamma\left(\frac{a}{2}+1\right) {}_2F_2\left(\frac{a}{2}+\frac{1}{2},\frac{a}{2}+1;\frac{1}{2},\frac{a}{2}+\frac{3}{2};\frac{1}{4b^2\bar{\gamma}q}\right) - (a+1)\Gamma\left(\frac{a+3}{2}\right){}_2F_2\left(\frac{a}{2}+1,\frac{a}{2}+\frac{3}{2};\frac{3}{2},\frac{a}{2}+2;\frac{1}{4b^2\bar{\gamma}q}\right)\right)}{2\sqrt{\pi}(a+1)(a+2)b^2\bar{\gamma}\Gamma(a+1)},$$

(14)

where $pF_q(a_1,...,a_p;b_1,...,b_q;x)$ is the generalized hypergeometric function [16, Eq. (9.14.1)].

$$C = \frac{1}{\ln(2)\Gamma(a+1)}\left(\frac{\Gamma(a-1){}_2F_3\left(1,1;2,1-\frac{a}{2},\frac{3}{2}-\frac{a}{2};-\frac{1}{4b^2\bar{\gamma}}\right)}{b^2\bar{\gamma}} + \frac{\pi b^{-a-2}\bar{\gamma}^{-\frac{a}{2}-1}\csc\left(\frac{\pi a}{2}\right){}_1F_2\left(\frac{a}{2}+1;\frac{3}{2},\frac{a}{2}+2;-\frac{1}{4b^2\bar{\gamma}}\right)}{a+2}\right.$$
$$\left.+\frac{\pi b^{-a-1}\bar{\gamma}^{-\frac{a}{2}-\frac{1}{2}}\sec\left(\frac{\pi a}{2}\right){}_1F_2\left(\frac{a}{2}+\frac{1}{2};\frac{1}{2},\frac{a}{2}+\frac{3}{2};-\frac{1}{4b^2\bar{\gamma}}\right)}{a+1} - 2a^2\Gamma(a-1)\ln\left(\frac{1}{b\sqrt{\bar{\gamma}}}\right) + 2a\Gamma(a-1)\ln\left(\frac{1}{b\sqrt{\bar{\gamma}}}\right) + 2(a-1)a\Gamma(a-1)\psi^{(0)}(a+1)\right),$$

(15)

where $\psi^0(.)$ gives the 0th polygamma function, which is the 0th derivative of the digamma function.

channels, G_d simplifies to $\frac{\pi^2 N}{32-2\pi^2}$. These results on G_c and G_d are new and being presented for the first time in literature. It is worthwhile to mention here that, in [12], the authors approximated G_d of RIS-assisted networks as that of MIMO channels $N-1 < G_d < N$. Here, we show that this only applies when N takes a value equal to 5 or less, but when N goes more than 5, G_d could get below the floor $N-1$.

B. Average Symbol Error Probability

The average symbol error probability (ASEP) can be expressed in terms of the CDF of γ as [19]

$$\text{ASEP} = \frac{p\sqrt{q}}{2\sqrt{\pi}}\int_0^\infty \frac{\exp(-q\gamma)}{\sqrt{\gamma}}F_\gamma(\gamma)d\gamma, \quad (16)$$

where p and q are modulation-specific parameters.

Theorem 2: The ASEP of RIS-assisted network assuming Nakagami-m fading model can be analytically obtained as in (14), given at the top of this page.

Proof: The proof is carried out by substituting (3) in (16). The integral is evaluated by substitution, then by parts, then by substitution again, and then the relation [20, Eq. 06.25.21.0131.01] is utilized. After doing some algebraic manipulations, the result given in (14) is obtained. ∎

The complete proof is not included due to space limitations, but can be provided upon request.

C. Average Channel Capacity

The average channel capacity can be expressed in terms of the PDF of γ as [21]

$$C = \frac{1}{\ln(2)}\int_0^\infty \ln(1+\gamma)f_\gamma(\gamma)d\gamma. \quad (17)$$

Theorem 3: The average channel capacity of RIS-assisted network assuming Nakagami-m fading model can be analytically obtained as in (15).

Proof: The proof is carried out by substituting (2) in (17). According to [22], the natural logarithmic function can be written in terms of hypergeometric function as follows

$$\ln(1+y) = y {}_2F_1(1,1;2;-y). \quad (18)$$

Employing this and using [20, Eq. 07.23.21.0015.01], the result given in (15) is obtained. ∎

IV. SIMULATION AND NUMERICAL RESULTS

Here, 15,000 iterations have been generated for each value of the SNR to calculate the outage probability. Furthermore, the BPSK modulation scheme ($p = q = 1$) has been used in the ASEP simulation results.

Fig. 1 shows that the derived analytical and asymptotic expressions are matching the simulation results, which validates the used analysis approach. In addition, we can see from this figure that N is noticeably affecting the diversity order of the system, which coincides with the derived diversity order in Section III. For example, 10 reflecting elements can be used instead of 5 to achieve an outage probability of 10^{-4} and save the average SNR by an amount of almost 11 dB. As expected, the asymptotic expressions match the analytical and simulation results at high average SNR values.
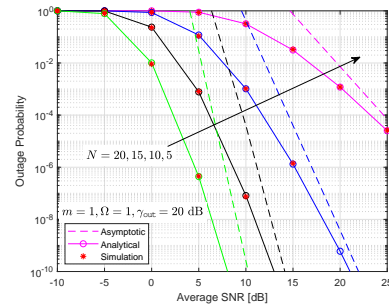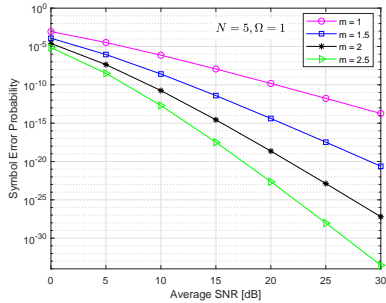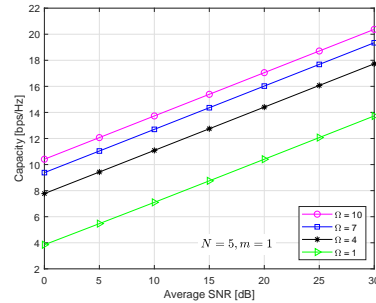

Fig. 1: P_{out} vs SNR for different values of N.

We can see from Fig. 2 that the fading parameter m is affecting the diversity order of the system G_d, where as m increases, G_d increases and better the achieved performance. This is expected, as m increases, the quality of the fading channel improves, and hence, better the system performance.

Fig. 3 portrays the diversity order of the system versus N for different values of m. The results are based on the asymptotic outage probability performance metric. We can see that the fading parameter m has higher impact on G_d, and hence, the system performance than the number of reflecting elements N. For example, a diversity order of $G_d = 8$ when $N = 10$ and $m = 1$, whereas, a diversity order of $G_d = 9.75$ is almost achieved when $N = 1$ and $m = 10$. This clearly shows that

Fig. 2: ASEP vs SNR for different values of m.
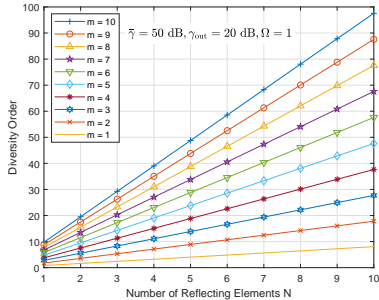
Fig. 3: G_d vs N for different values of m.

G_d could go below than $mN - 1$ by a big amount when N is larger than m, especially at high values of N and m, but is almost floored by $Nm - 1$ when m is larger than N even at high values of N and m.

Fig. 4 studies the effect of Ω on the system performance. It is obvious from this figure that as Ω increases, better the achieved capacity. In addition, we can see that as Ω continues increasing, the gain achieved in system capacity gets smaller.

V. CONCLUSION

This letter derived accurate closed-form approximations for the outage probability, ASEP, and the average channel capacity of RIS-assisted networks over Nakagami-m fading channels. In addition, it studied the outage probability performance at high SNR values, where the system diversity order and coding gain were derived and analyzed. Results showed that the considered RIS scenario can provide a diversity order of $\frac{a+1}{2}$, where a is a function of the Nakagami-m fading parameter m and the number of reflecting elements N. Furthermore, results illustrated that m is more impactful on the system diversity order and the system performance than N.

REFERENCES

[1] M. Di Renzo *et al.*, "Reconfigurable intelligent surfaces vs. relaying: Differences, similarities, and performance comparison," *IEEE Access*, vol. 1, pp. 798–807, 2020.

[2] E. Basar, M. Di Renzo, J. De Rosny, M. Debbah, M.-S. Alouini, and R. Zhang, "Wireless communications through reconfigurable intelligent surfaces," *IEEE Access*, vol. 7, pp. 116753–116773, 2019.

[3] Y. Liang, R. Long, Q. Zhang, J. Chen, H. V. Cheng, and H. Guo, "Large intelligent surface/antennas (LISA): making reflective radios smart," *J. Commun. Netw-S. Kor.*, vol. 4, no. 2, pp. 40–50, June 2019.

[4] E. Basar, M. Di Renzo, J. De Rosny, M. Debbah, M.-S. Alouini, and R. Zhang, "Wireless communications through reconfigurable intelligent surfaces," *IEEE Access*, vol. 7, pp. 116753–116773, June 2019.

Fig. 4: Capacity vs SNR for different values of Ω.

[5] Q. Wu, and R. Zhang, "Intelligent reflecting surface enhanced wireless network via joint active and passive beamforming," *IEEE Trans. Wireless Commun.*, vol. 18, no. 11, pp. 5394–5409, Nov. 2019.

[6] L. Yang, X. Yan, D. B. D. Costa, T. A. Tsiftsis, H.-C. Yang, and M.-S. Alouini, "Indoor mixed fual-hop VLC/RF systems through reconfigurable intelligent surfaces," *IEEE Commun. Lett.*, Early Access, DOI 10.1109/LWC.2020.3010809.

[7] L. Yang , Y. Yang, M. O. Hasna, and M.-S. Alouini, "Coverage, probability of SNR gain, and DOR analysis of RIS-aided communication systems," *IEEE Wireless Commun. Lett.*, vol. 9, no. 8, pp. 1268–1272, Aug. 2020.

[8] L. Yang, W. Guo, and I. S. Ansari, "Mixed dual-hop FSO-RF communication systems through reconfigurable intelligent surface," *IEEE Commun. Lett.*, vol. 24, no. 7, pp. 1558–1562, July 2020.

[9] L. Yang, F. Meng, J. Zhang, M. O. Hasna, and M. D. Renzo, "On the performance of RIS-assisted dual-hop UAV communication systems," *IEEE Trans. Veh. Technol.*, Early Access, DOI 10.1109/TVT.2020.3004598.

[10] A. E. Canbilen, E. Basar, and S. S. Ikki, "Reconfigurable intelligent surface-assisted space shift keying," *IEEE Commun. Lett.*, Early Access, DOI 10.1109/LWC.2020.2994930.

[11] L. Yang, J. Yang, W. Xie, M. O. Hasna, T. Tsiftsis, and M. D. Renzo, "Secrecy performance analysis of RIS-aided wireless communication systems," *IEEE Trans. Veh. Technol.*, Early Access, DOI 10.1109/TVT.2020.3007521.

[12] L. Yang, F. Meng, Q. Wu, D. B. D. Costa, and M.-S. Alouini, "Accurate closed-form approximations to channel distributions of RIS-aided wireless systems," *IEEE Commun. Lett.*, Early Access, DOI 10.1109/LWC.2020.3010512.

[13] A.-A. A. Boulogeorgos and A. Alexiou, "Performance analysis of reconfigurable intelligent surface-assisted wireless systems and comparison with relaying," *IEEE Access*, vol. 8, pp. 94463–94483, 2020.

[14] R. C. Ferreira1, M. S. P. Facina1, F. A. P. D. Figueiredo, G. Fraidenraich, and E. R. D. Lima, "Bit error probability for large intelligent surfaces under double-Nakagami fading channels," *IEEE Open J. Commun. Soc.*, vol. 1, pp. 750–759, June 2020.

[15] S. Primak, V. Kontorovich, and V. Lyandres, *Stochastic Methods and their Applications to Communications: Stochastic Differential Equations Approach*, West Sussex, U.K.: Wiley, 2004.

[16] I. S. Gradshteyn and I. M. Ryzhik, *Tables of Integrals, Series and Products*, 6th ed., San Diago: Academic Press, 2000.

[17] M. Abramowitz and I. A. Stegun, *Handbook of Mathematical Functions with Formulas, Graphs, and Mathematical Tables*, 9th ed., New York, NY, USA: Dover, 1972.

[18] M. K. Simon and M.-S. Alouini, *Digital Communication over Fading Channels*, 2nd ed., Wiley, 2005.

[19] M. R. McKay, A. L. Grant, and I. B. Collings, "Performance analysis of MIMO-MRC in double-correlated Rayleigh environments," *IEEE Trans. Commun.*, vol. 55, pp. 497–507, March 2007.

[20] Wolfram, "The Wolfram functions site," Available: http://functions.wolfram.com/06.25.21.0131.01 .

[21] J. Vellakudiyan, I. S. Ansari, V. Palliyembil, P. Muthuchidambaranathan, and K. A. Qaraqe, "Channel capacity analysis of a mixed dual-hop radio-frequency-free space optical transmission system with Mlaga distribution," *IET Commun.*, vol. 10, pp. 2119–2124, Oct. 2016.

[22] Wikipedia contributors, "Hypergeometric function". In Wikipedia, The Free Encyclopedia. Retrieved 17:37, October 14, 2020, from https://en.wikipedia.org/w/index.php?title=Hypergeometric function & oldid=978101645.